

# Phonons in large-band-gap materials

M. Schwoerer-Böhning

*Carnegie Institution of Washington, c/o Advanced Photon Source, 9700 S. Cass Ave., Argonne, IL 60439 USA*

A.T. Macrander

*Advanced Photon Source, Experimental Facilities Division, 9700 S. Cass Ave., Argonne, IL 60439 USA*

The outstanding thermal and chemical stability of large-band-gap materials (e.g., silicon carbide and III–V nitride semiconductors) make these materials promising candidates for high-temperature electronics and short-wavelength optical applications. We present first studies of the phonon dispersion in hexagonal silicon carbide along the  $\Gamma$ - $K$ - $M$  direction and in hexagonal aluminum nitride along all three high-symmetry directions. Investigating the lattice dynamics of small single crystals (volume  $\leq 1 \text{ mm}^3$ ) has become feasible with the advent of high-resolution inelastic x-ray scattering.

Electronics based on the existing semiconductor device technologies of Si and GaAs cannot tolerate greatly elevated temperatures or chemically hostile environments due to the uncontrolled generation of intrinsic carriers and the low resistance to caustic chemicals. However, wide-band-gap materials with their high-temperature stability and corrosion resistance seem to be excellent candidates for high-power operations in aerospace, automotive, and petroleum industries.

SiC, in particular, exists in a variety of long-range-ordered structures, the so-called polytypes. Theoretical work, therefore, focuses on the mechanism that leads to the various polytypes [1]. Since the electronic energies of the different phases of SiC are very close, the phonon contributions to the free energy could be important. A reliable test of various model calculations is the study of the phonon dispersions and the band structure. Macrander *et al.* measured electronic excitations in 6H-SiC by means of inelastic x-ray scattering along high-symmetry lattice directions [2]. However, there is still not enough evidence to indicate whether band-structure calculations in the local density approximation can explain the polytypism. Various attempts have been made to calculate the phonon dispersions in SiC of zinc-blende structure. Karch *et al.* presented first-principles calculations of the phonon dispersions in the 2H and 4H phases [3]. Based on the bond-charge model, a phenomenological approach by Hofmann *et al.* has achieved excellent agreement with experimental data [4].

Wurtzite AlN is similar to SiC. It belongs to the III–V nitrides and together with GaN attracts attention as a material used for blue lasers. While wurtzite AlN is available in single crystals large enough ( $> 1 \text{ mm}^3$ ) [5, 6] for inelastic x-ray scattering studies, GaN single crystals of

reasonable size are difficult to grow. Investigating the lattice dynamics of AlN is the first step to the understanding of GaN and InN. The last two require modified theoretical models due to the presence of 3d and 4d electrons, respectively [5]. The current conclusion is that among the III–V nitrides, the zinc-blende structure is more favorable for doping than the wurtzite structure and, therefore, theoretical work has focused on the lattice dynamics of the zinc-blende structure [7–9]. To our knowledge, experimental work related to phonon dispersions in wurtzite AlN has been done on powdered samples only. Recently, Nipko *et al.* measured the phonon density of states with inelastic neutron scattering (INS) [10]. Applying a rigid-ion model, the phonon density of states derived from calculated phonon dispersions agrees well with their data. In [8], Karch *et al.* present phonon dispersions of zinc-blende AlN resulting from first-principles calculations. They are considerably different from the results calculated by Zi *et al.* [9]. Besides differences in the calculated frequencies, a pronounced feature in the results of [9] does not occur in the work by Karch *et al.* [7, 8]. Zi *et al.* achieve a mixing of the transverse and longitudinal branch along the  $\langle 110 \rangle$  direction.

The recently developed instrument for high-resolution inelastic x-ray scattering (HRIXS) at the Advanced Photon Source (APS) is located at sector 3 of the Synchrotron Radiation Instrumentation Collaborative Access Team (SRI-CAT) [11]. The insertion device of the undulator beamline provides a typical photon flux of  $3 \times 10^9$  photons/s within a band pass of approximately 5 meV at a photon energy of 13.8 keV. The data were taken with a total energy resolution of approximately 9 meV. In addition to the instrumental energy resolution of 8 meV, one must account for the contribution from the sample mosaic. Details about the instrument can be found in [11]. The SiC single crystal was approximately  $4 \times 4 \text{ mm}^2$  and 0.5 mm thin. Measurements were done in the Laue geometry with the  $\langle 110 \rangle$  direction parallel to the flat face of the crystal. The width of the (220) reflection in a rocking scan was 0.003 degrees. The longitudinal polarized phonon dispersion was measured in the momentum transfer range of  $Q = 0.85$  to  $Q = 2.1 \text{ 2}\pi/\text{d}$ . Raw phonon spectra are presented in Figure 1. The scattering yield ranges up to 50 photons/s. The energy resolution does not resolve well the phonons at  $Q = 1.3 [2 \pi/\text{d}]$  ( $K$ -point). Phonons of higher frequencies are strongly damped. Elastic scattering is from imperfections in the crystal and from a Kapton foil attached to the sample

which provides the zero energy transfer for calibration at any momentum transfer.

The complete data set in Figure 2 was collected within 12 hours of beam time. The error in the phonon energy is of the order of the symbol size.

The AlN single crystal was of hexagonal shape and approximately 0.5 x 0.5 x 0.5 mm. Like SiC, the measurements on AlN were also done in transmission. Typical raw data are shown in figure 3. Longitudinal and transverse polarized phonons were studied along  $\langle 001 \rangle$ ,  $\langle 100 \rangle$ , and  $\langle 110 \rangle$  ( $\Gamma$ -A,  $\Gamma$ -M, and  $\Gamma$ -K-M) directions in the (006), (300), and (220) zones. The typical width of Bragg reflections was a few hundredths of a degree. The data collection took four days. The complete set of measured dispersion curves is presented in Figure 4. The lines in Figure 4 are to guide the eye.

The group of D. Strauch [12] has conducted INS studies on SiC at the high-intensity neutron source of the Institute Laue Langevin (ILL). Difficulties arise due to the poor quality of the larger crystals required for such experiments. Therefore, we present first results on the dispersion of longitudinal phonons along  $\Gamma$ -K-M. To our knowledge, only the work by Hofmann *et al.* [4] presents calculations of the phonon dispersions in 6H-SiC. Comparing critical point energies of our work with the work by Hofmann *et al.* we find excellent agreement. The measured energies of the acoustic and optic branch at the K-point, 67 meV and 60 meV, correspond to the calculated wave numbers of 536  $\text{cm}^{-1}$  and 480  $\text{cm}^{-1}$ , respectively. The flat dispersions of the upper optical branches at 95 meV and 105 meV agree well with the calculated frequencies of 750  $\text{cm}^{-1}$  and 850  $\text{cm}^{-1}$  at the M-point. Our work demonstrates that HRIXS studies on SiC can provide knowledge about the important lattice dynamics in SiC polytypes.

In the case of AlN we cannot refer to first-principles calculations of phonon dispersions in wurtzite AlN. The rigid-ion model calculations by Nipko and Loong are the only available results of phonon dispersions in hexagonal AlN. Comparing the calculated dispersions along  $\lambda$  in the work by Karch *et al.* and Zi *et al.* with the results along  $\Delta$  calculated by Nipko and Loong, we find already a significant difference for the phonon frequencies (energies) both at L (zinc-blende) and  $\Gamma$  (wurtzite). For the longitudinal polarized acoustic (LA) phonon in wurtzite at  $\Gamma$  the following values have been reported: 501  $\text{cm}^{-1}$  [9], 574  $\text{cm}^{-1}$  (Karch *et al.*), and 560  $\text{cm}^{-1}$  [10]. Our data reveal  $73 \pm 1$  meV which is equal to  $584 \pm 8$   $\text{cm}^{-1}$ . The lower energy of the LO ( $\Delta$ )phonon at  $\Gamma$  measured in our experiment agrees well with the calculated energy in all three references, while the upper value of 120 meV (960  $\text{cm}^{-1}$ ) lies far above calculated energies: 98 meV [10], 113 meV [9], and 114 meV (Karch *et al.*). Overall, our data are in good agreement

with calculated phonon dispersions. The instrument could not resolve all optical branches. A major difference between experiment and theory occurs in the transverse polarized acoustic (TA) phonons along  $\Sigma$  and  $T$  ( $\Gamma$ -K-M- $\Gamma$ ). In the theoretical work by Nipko and Loong, different phonon energies for in-plane and out-of-plane polarized TA phonons occur. However, in our work there is no difference between TA phonons along both directions. The dispersions appear rather like the TA phonon dispersions in zinc-blende structure [8, 9]. A similar difference occurs in the calculated phonon dispersions of 3C and 2H-SiC [4]. The lack of agreement between our data and the rigid-ion model calculations might be related to that the model does not account for the polarizability of the atoms.

## Acknowledgments

We thank SRI-CAT staff of sector 3 for the performance of the beamline. We are also indebted to the management of the Experimental Facilities Division at APS. P.A. Montano has lent us the SiC sample, and the AlN crystal was borrowed from C.M. Balkas. Use of the APS was supported by the U.S. Department of Energy, Basic Energy Sciences, Office of Science, under Contract No. W-31-109-ENG-38.

Reprinted, Journal of Physics and Chemistry of Solids, Vol. 61, M. Schwoerer-Bohning and A.T. Macrander, "Phonons in large-band-gap materials", pp. 485–487, Copyright 2000), with permission from Elsevier Science.

## References

- [1] in W.J. Choyke, H. Matsunami, and G. Pensl, editors, *Physica Status Solidi (b)* **202**, (1997).
- [2] A.T. Macrander, R.C. Blasdel, P.A. Montano, and C.C. Kao, in *Wide Bandgap Semiconductors and Devices and 23rd State-of-the-Art Program on Compound Semiconductors, Electrochemical Society Proceedings*, Ren *et al.*, editors, **95–21**, 98ff, (1995).
- [3] K. Karch, P. Pavone, W. Windl, O. Schütt, and D. Strauch, *Phys. Rev. B* **50**, 17054 (1994).
- [4] M. Hofmann, A. Zywietz, K. Karch, and F. Bechstedt. *Phys. Rev. B* **50**, 13401 (1994).
- [5] C.M. Balkas, Z. Sitar, T. Zheleva, L. Bergman, R. Nemanich, and R.F. Davis, *J. Crystal Growth* **179**, 363 (1997).
- [6] M. Tanaka, S. Nakahata, K. Sogabe, H. Nakata, and M. Tobioka, *Jpn. J. Appl. Phys.* **36**, L1062 (1997).
- [7] K. Karch, F. Bechstedt, and T. Pletl, *Phys. Rev. B* **56** 3560, (1997).
- [8] K. Karch, F. Bechstedt, P. Pavone, and D. Strauch, *Physica B* **219 and 220**, 445 (1996).
- [9] J. Zi, X. Wan, G. Wei, K. Zhang, and X. Xie, *J. Phys. C* **8**, 6323 (1996).
- [10] J.C. Nipko, and C.K. Loong, *Phys. Rev. B* **57**, 10550 (1998).

- [11] M.Schwoerer-Böhning, A.T. Macrander, P.M. Abbamonte, and D.A. Arms, *Rev. Sci. Instrum.* **69**, 3109 (1998).  
 [12] D.Strauch. (private communication).

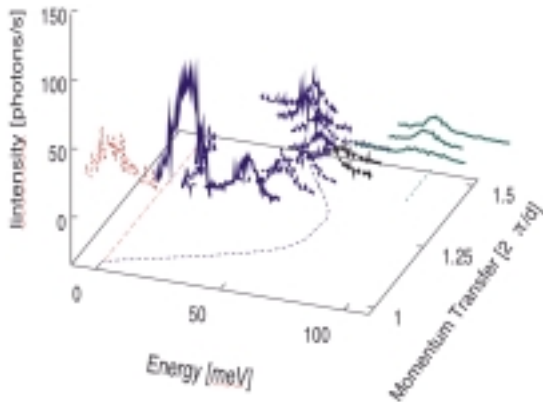


Figure 1: Phonon spectra along  $\Gamma$ -K-M in 6H-SiC.

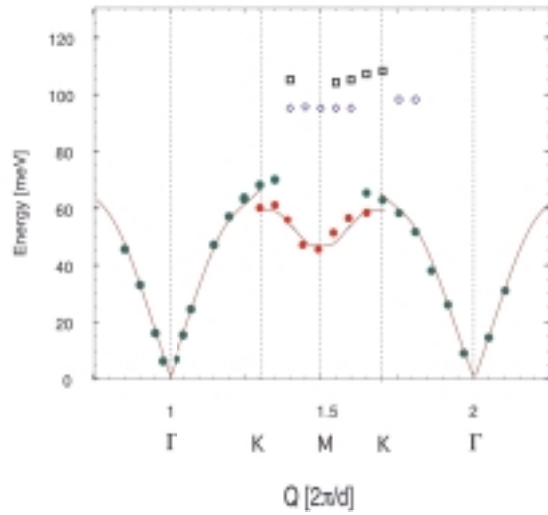


Figure 2: Longitudinal phonon dispersions of 6H-SiC along  $\Gamma$ -K-M, acoustic and optic branches (the lines are to guide the eyes).

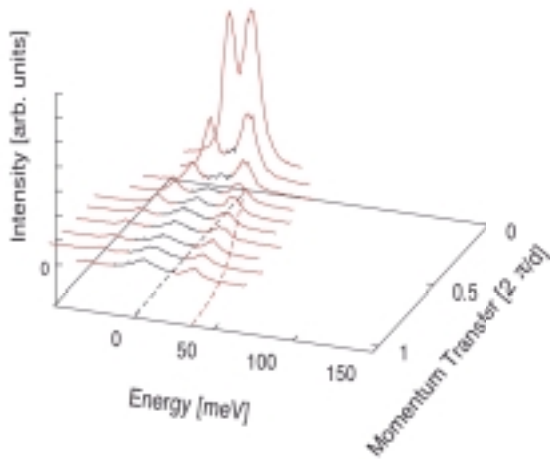


Figure 3: Transverse phonon spectra along  $\Gamma$ -A in hcp-AlN.

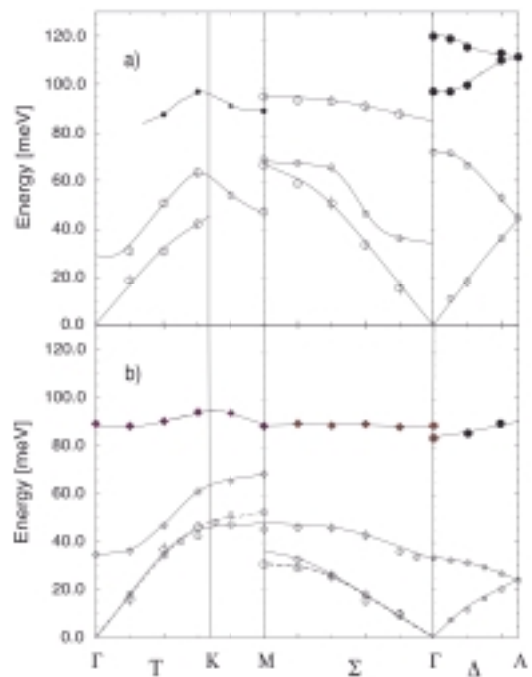


Figure 4: Longitudinal a) and transverse b) polarized phonon branches in hcp-AlN (the lines are to guide the eyes).